



Next Generation Very Large Array Memo No. 11 Imaging Capabilities: Protoplanetary disks Comparison of ngVLA, JVLA, ALMA

C.L. Carilli^{1,4}, L. Ricci², P. Barge³, B. Clark¹

Abstract

We perform simulations of the capabilities of the Next Generation Very Large Array in the context of imaging the terrestrial zone of protoplanetary disks. We use as a test image the protoplanetary disk model of Barge, Ricci, & Previn (2016), at the distance of the Rho Ophiuchi cloud complex. We adopt a fiducial configuration with 30% of the antennas within a 1km radius, and maximum baselines of 300km. Imaging with this configuration (with robust = 0.5), achieves 12mas resolution at 30GHz, and a sensitivity of $0.04\mu\text{Jy beam}^{-1}$ in 100hours, corresponding to a brightness temperature sensitivity of 0.4K. The corresponding numbers at 80GHz are 5mas and $0.11\mu\text{Jy beam}^{-1}$. We then compare these results with what can be done with the current JVLA and ALMA. Tapered to the resolution of the JVLA at 30GHz (60mas), the noise level for the ngVLA is $0.074\mu\text{Jy beam}^{-1}$, roughly 7.5x more sensitive than the JVLA at matched resolution. Tapering to the ALMA Band 1 resolution at 30GHz (130mas), yields a sensitivity for the ngVLA of $0.09\mu\text{Jy beam}^{-1}$, a factor of 6.7 better than ALMA at matched resolution. A similar comparison is made at 80GHz between the ngVLA and ALMA Band 3. These simulations indicate that the ngVLA will perform revolutionary imaging of the terrestrial zone of planet formation on sub-AU scales, in common, dusty protoplanetary disks at the distance of Rho Ophiuchus, Taurus, and other well studied star forming regions.

¹NRAO, PO Box O, Socorro, NM

²Harvard-Smithsonian Center for Astrophysics, Cambridge, MA

³Aix-Marseille-Universite CNRS Laboratoire d'Astrophysique de Marseille UMR 7326, F-13013 Marseille, France

⁴Cavendish Astrophysics Group, Cambridge University, Cambridge, UK

1 Introduction

The ‘Next Generation Very Large Array’ (ngVLA), is currently being designed as a future large radio facility operating in the 1GHz to 115GHz range. The current design involves ten times the effective collecting area of the JVLA and ALMA, with ten times longer baselines (300km) providing mas-resolution, plus a dense core on km-scales for high surface brightness imaging. The ngVLA opens unique new parameter space in the imaging of thermal emission from cosmic objects ranging from protoplanetary disks to distant galaxies, as well as unprecedented broad band continuum polarimetric imaging of non-thermal processes (Carilli et al. 2015).

One of prime science drivers for the ngVLA involves making order-of-magnitude improvements in the study of planet formation through imaging of dusty protoplanetary disks at 5mas to 10mas resolution (Isella et al. 2015). This resolution corresponds to about 1AU at a distance 140pc \sim the distance to the nearest star forming regions, such as Rho Ophiuchus and Taurus. Moreover, the ngVLA probes frequencies at which the inner dusty disks in young proto-planetary regions (\sim few Myr old), are optically thin in the dust continuum, with adequate sensitivity to detect the inner dust structures at full resolution. Hence, the ngVLA will be the premier instrument to study planet formation in the terrestrial zone, otherwise unobservable at shorter (submm) wavelengths due to dust opacity.

In this memo, we investigate the ngVLA capabilities in the area of terrestrial-zone planet formation, and compare these capabilities with those of existing facilities. Specifically, we compare the ngVLA capabilities at 80GHz with the current ALMA in its most extended configuration (‘out28’ = 15km maximum baselines). We also compare ngVLA capabilities at 30GHz with the current A configuration of the JVLA, and with the future ALMA band 1 in the out28 configuration.

We focus on the basic parameters of sensitivity, resolution, and examples of image quality. As a test case, we employ the protoplanetary disk model of Barge, Ricci, Previn (2016), described in Section 2.

2 Protoplanetary Disk Model

Figure 1 shows the model sampled at 1mas per pixel at 30GHz, along with the ngVLA image at 30GHz at 12mas resolution (see section 5).

Two-dimensional numerical simulations were performed for the model of a young circumstellar disk that includes a giant gaseous vortex by Barge,

Ricci, & Previn (2016). They used a bifluid code to describe the coupled evolution of gas and dust. The disk parameters were adapted to the case of Oph-IRS 48, a young disk with a very strong azimuthal asymmetry as seen by ALMA at sub-millimeter wavelengths, likely due to the presence of a giant gaseous vortex at about 60 AU from the central star.

Several simulations were run for various particles sizes that range from 0.1mm to 2cm, in a ring between 20 and 100 AU from the star. For the sake of our array imaging demonstration, we show only the 2cm dust simulation. The numerical resolution is high enough to follow the confinement of the particles inside the vortex, and integration times were chosen long enough to follow significant changes in the distribution of the dust grains. The gas vortex itself is located close to the brightest spot on the ring in the 80GHz image.

The results of these simulations show clear differences between the dust evolution of solids with different sizes. Small particles (1mm), are very effectively captured and confined in the vortex, hence the bright spot in the 80GHz image close to the vortex itself.

Larger, 1cm-sized particles are captured and assembled in "blobs" in the vortex. These blobs are then progressively stripped out of the vortex due to differential forces that act preferentially on the large grains. Collective drag effects on the dust particles tend to maintain some coherence in the clustered particles. As a result, these large dust particles tend to form a narrow ring structure at the vortex orbital radius, punctuated by bright knots of emission.

Observations of disks at different wavelengths in the sub-mm to radio regimes have the capabilities to probe solids with different sizes in the disk, with larger grains being probed by observations at longer wavelengths. In the case of the simulations discussed herein, the behaviour of the "large particles" are best traced by sensitive observations in the dust continuum at short cm wavelengths.

Note that, although the simulations were broadly adapted to the case of Oph-IRS 48 (van der Marel et al. 2013), the goal was not to reproduce in detail the exact characteristics of the Oph-IRS 48 disk but rather to study the possible observational features that could be expected as a result of the mutual interaction between gas and solids in a disk with a giant gas vortex. For the purposes of this memo, the emphasis is on array capabilities, not on testing the physics of the particular model. The model simply represents a plausible, astrophysically interesting, test-bed for exploring array performance.

3 Configuration

Brightness sensitivity for an array is critically dependent on the array configuration. We are assuming an array of 300 antennas in this current configuration. The ngVLA has the competing desires of both good point source sensitivity at full resolution for few hundred km baselines, and good surface brightness sensitivity on scales approaching the primary beam size. Clark & Brisken (2015) explore different array configurations that might provide a reasonable compromise through judicious weighting of the visibilities for a given application. It is important to recognize the fact that for any given observation, from full resolution imaging of small fields, to imaging structure on scales approaching that of the primary beam, some compromise will have to be accepted.

For the numbers in Table 1, we have used the Clark-Conway configurations described in ngVLA memos 2 and 3, with some modifications. Briefly, this array entails a series of concentric 'fat-ring' configurations out to a maximum baseline of 300km. About 60% of the full array is within 15km radius, and 30% of the area within 1km radius. The inner core positions of antennas in the inner 1km have been randomized for better uv-coverage.

The configuration will be a primary area for investigation in the coming years. In particular, station locations will be strongly dictated by practical issues such as access, power, and fiber. The main goal herein is to investigate high resolution imaging in the case of an array with a substantial short-spacing core. We have investigated different Briggs weighting schemes for specific science applications, and find that the Clark/Conway configuration provides a reasonable starting compromise for further calculation.

For the JVLA we used the A configuration available in the CASA tool kit, for which the maximum baseline is 30km. For ALMA, we used the most extended configuration currently planned for full operations (15km maximum baseline), available as the 'alma.out28.cfg' configuration in the CASA tools.

4 Mechanics of the simulation

We employed the SIMOBSERVE task within CASA to generate uv data sets. The input models were from numerical simulations of the Barge et al. (2016) protoplanetary disk, as described in Section 2. The models were in FITS format, with brightness units of Jy pixel^{-1} , all sampled at 1mas pixel size to avoid questions of losing information due to the sampling of the input

image.

The FITS headers were adjusted to allow for proper execution of `simobserve`, including RA/Dec projection (eg. 'RA—SIN'), frequency and Stokes entries, and brightness units. In order to obtain a fair comparison of the imaging capabilities, we adjusted the declination of the source to be -24° for ALMA, and $+24^\circ$ for the ngVLA and JVLA.

The simulated observation entailed a 4hour synthesis centered on transit. Due to operational intricacies, `simobserve` was not used to set the noise per visibility. Thermal noise was added to the visibilities after the fact using the CASA tool `SETNOISE`. The noise per visibility was scaled to obtain a final image rms that would correspond to a 100 hour integration for each facility. Bandwidths are given in Table 1. For ALMA and the JVLA, the available sensitivity calculators were used. For the ngVLA, we used system parameters as given in Table 1 of Carilli et al. (2015). Note that we assumed the full bandwidth for the noise calculation, but we did not employ bandwidth synthesis for imaging due complexities in simulation and imaging. Improved uv-coverage with bandwidth synthesis should improve imaging capabilities.

In all cases we employed the CLEAN algorithm with Briggs weighting with $R = 0.5$. We also employed a multiscale clean approach, due to the existence of both high brightness, and large, diffuse structures in the model. Images were generated at full spatial resolution for each array.

Lastly, we generate tapered images from the ngVLA data with restoring beams approximately matched to the JVLA and ALMA resolutions. These allow for a detailed comparison of the capabilities at matched resolution.

5 Results

The results are summarized in Table 1.

At 30GHz, the current JVLA and the future ALMA Band 1, have similar sensitivities to each other (ie. comparable effective collecting area and bandwidth), while the JVLA A configuration has twice the spatial resolution of the most extended ALMA configuration.

5.1 30GHz model

Figure 2 shows the disk image at 30GHz at the full spatial resolution of each array, corresponding to 12mas, 60mas, and 130mas for the ngVLA, the JVLA, and ALMA Band 1, respectively. Note that by using Briggs

Table 1: Imaging with the ngVLA, JVLA, ALMA

	Resolution ^a	Sensitivity ^a	Peak	Bandwidth	B _{short} ^b	S _{short} ^c	B _{long}
	milliarcsec	$\mu\text{Jy beam}^{-1}$	$\mu\text{Jy beam}^{-1}$	GHz	meters	mJy	km
ngVLA30GHz	12	0.040	9.4	20	25	0.15	300
ngVLA30GHz TA-VLA ^d	67	0.073	16.8	–	–	–	–
ngVLA30GHz TA-ALMA ^e	120	0.090	21.6	–	–	–	–
ngVLA80GHz	5	0.11	18.0	30	–	2.4	–
ngVLA80GHz TA-ALMA	55	0.17	442	–	–	–	–
JVLA-A 30GHz	60	0.55	16.5	8	700	0.12	30
ALMA-out28 30GHz	130	0.60	23.7	8	100	0.15	15
ALMA-out28 80GHz	50	0.92	417	8	–	2.4	–

^aFWHM and rms noise for Briggs weighting with $R = 0.5$, 100hr integration, $\Delta\text{HA} = \pm 2\text{hr}$

^bShortest baseline in array (A array for JVLA, out28 for ALMA)

^cFlux density on shortest baseline

^dngVLA tapered to JVLA resolution

^engVLA tapered to ALMA resolution

weighting with $R=0.5$ in the imaging, we sacrifice some spatial resolution for each array, in order to obtain reasonable noise levels.

The 10x more sensitive, and 10x higher spatial resolution of the ngVLA shows structure in the narrow dust ring of the model in exquisite detail, down to $\sim 1.7\text{AU}$ scales. The ngVLA reaches a noise level of 40nJy beam^{-1} . This corresponds to a brightness temperature limit of 0.4K at 12mas resolution. Even at this high spatial resolution, the lower surface brightness, broader dust disk, and the central dusty regions obscuring the star itself, are visible in the ngVLA image, although better imaged using a uv-taper (see Figure 3). The brightest emission in the ring is $9.4\mu\text{Jy beam}^{-1}$, or 90K .

The JVLA image reveals the brighter, narrow ring in some detail, but is not sensitive enough to pick up the lower surface brightness disk, even at this lower spatial resolution. The ALMA image also detects the bright ring, but the details of the structure are further blurred, and again, the low surface brightness disk is difficult to see.

We consider ngVLA imaging using tapers to approximate the resolution of ALMA and the JVLA. Figure 3 shows the comparison of the ngVLA tapered image and the JVLA image at $\sim 60\text{mas}$ resolution. Even tapered to 67mas resolution, the ngVLA obtains a noise level of 73nJy beam^{-1} , or a factor 7.5 better than the JVLA. The diffuse emission from the disk is clearly detected, as is the dust surrounding the central star.

Figure 4 shows the comparison of the ngVLA tapered image and the

ALMA image at ~ 130 mas resolution. The ngVLA noise level is 90nJy beam^{-1} at this taper, or a factor 6.7 better than for ALMA. The diffuse emission from the disk and the dust region at the center surrounding the star are now well detected and imaged at this resolution.

Note that the total flux density in the model at 30GHz is 0.15mJy , with a maximum size of about $1.5''$. The shortest spacings of the ngVLA detect all of this emission (Column 7, Table 1). The shortest baselines in the ALMA-out128 configuration also detect all the flux, although the low surface brightness of the diffuse disk is difficult to image at full resolution with ALMA due to limited sensitivity. The JVLA A configuration only gets 0.12mJy on the shortest baselines, requiring the need for more compact configurations to detect the diffuse disk.

Figure 5 shows a blow-up of the bright arc at 30GHz with the ngVLA at the full spatial resolution of 12mas. Again, multiple structures are imaged down to scales of 1.7AU. In the model, these bright knots at 30GHz correspond to aggregates of large (1cm) sized dust grains stripped out of the gas vortex, forming a bright ring at the radius of the vortex.

5.2 80GHz model

Figure 6 shows the disk image at 80GHz at the full spatial resolution of each array, corresponding to 5mas and 50mas for the ngVLA and ALMA, respectively. The ngVLA reaches a noise level of $0.11\mu\text{Jy beam}^{-1}$, or a brightness temperature limit of 0.65K. The brightest region is $18\mu\text{Jy beam}^{-1}$, or 106K.

At 80GHz, the ring becomes a bright arc centered on the vortex. This morphology arises due to the greater confinement of small dust grains to the vicinity of the vortex, while aggregates of larger grains migrate away from the vortex along the ring.

The arc has peak surface brightness of $18\mu\text{Jy beam}^{-1}$. The diffuse disk and inner dust region around the star, are clearly visible, but highly over-resolved. ALMA detects the arc, as well diffuse emission associated with the arc, but the diffuse disk is barely visible.

Figure 7 shows the ngVLA image tapered to ALMA resolution (55mas). The noise level is now $0.17\mu\text{Jy beam}^{-1}$, or a factor 5.4 better than ALMA. The diffuse emission from the disk is well imaged, as is the dust region at the center surrounding the star.

The total flux density in the model is 2.4mJy , and the short spacings of both ALMA and the ngVLA see all of this emission.

Figure 8 shows a blow-up of the bright arc at 80GHz with the ngVLA at 5mas resolution. Multiple linear and compact structures are imaged down

to scales of 0.7AU.

6 Conclusions

These simulations of the Next Generation Very Large Array show the power of imaging at short centimeter and long millimeter wavelengths in the study of planet formation. ALMA and the JVLA can, and certainly are, making excellent progress in studies of planet formation in dusty disks (eg. Carrasco-Gonzalez et al. 2016; Brogan et al. 2015; Andrews et al. 2016). However, the order of magnitude improvement in both spatial resolution and sensitivity of a facility such as the ngVLA operating in the 0.3cm to 1cm range, is required to probe down to sub-AU scales in the 'terrestrial zone' of planet formation – regions that are typically optically obscured at submm wavelengths.

Acknowledgments

The National Radio Astronomy Observatory is a facility of the National Science Foundation operated under cooperative agreement by Associated Universities, Inc. We thank Remy Indebetouw for help with simobserve.

References

- Andrews, S. et al. 2016, *ApJ*, 820, L40
Barge, Ricci, & Previn 2016, in prep.
Brogan, C. et al. 2015, *ApJ*, 808, L4
Carilli, C. et al. 2015, *NGVLA Memo. 5: Project Overview* (arXiv:1510.06438)
Clark, B. & Briske, W. 2015, *Next Generation VLA memo. No. 3*
Clark, B. 2015, *Next Generation VLA memo. No. 2*
Carrasco-Gonzalez, C. et al. 2016, *ApJ*, in press (arXiv:1603.03731)
Isella, A. et al. 2015, *Next Generation VLA memo. No. 6: the Cradle of Life* (arXiv:1510.06444)
ven der Marel et al. 2013, *Science* 340, 1199.

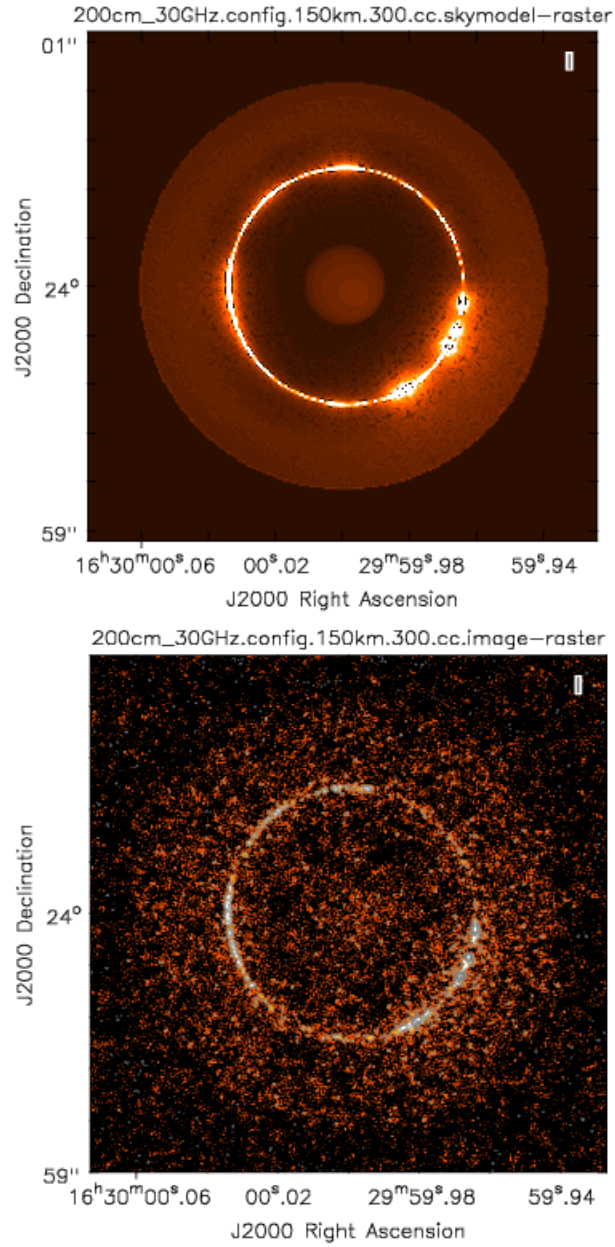


Figure 1: *Simulated images at 30GHz of the Barge et al. protoplanetary disk model at 140pc distance. Top: The model at 1mas per pixel and no noise nor convolving beam. Bottom: The Next Generation Very Large Array image at 12mas resolution with an integration time of 100hours, implying an rms noise of $40nJy \text{ beam}^{-1}$.*

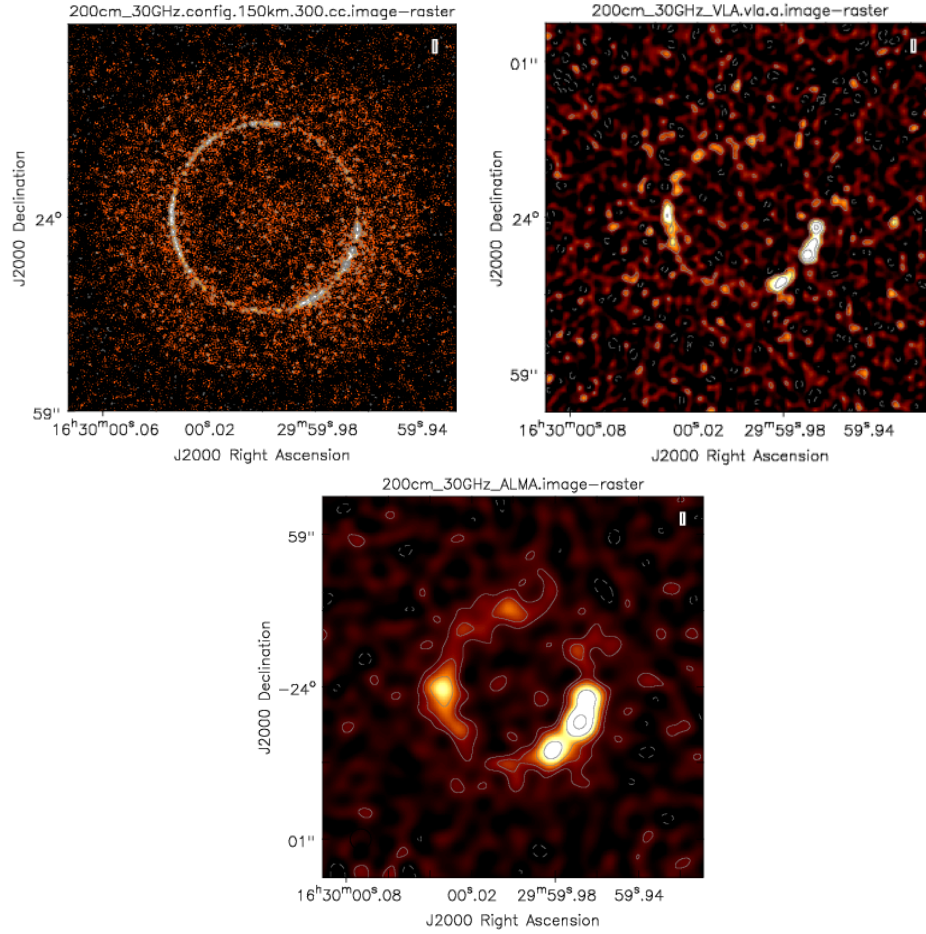


Figure 2: Simulated images at 30GHz of the Barge et al. protoplanetary disk model at a 140pc distance. Top: The Next Generation Very Large Array image at 12mas resolution. Center: The Jansky Very Large Array A array simulation of the same disk, at 67mas resolution. Bottom: The Atacama Large Millimeter Array 'out28 configuration' image of the disk at 120mas resolution. In all cases, the integration time is 100hours. The rms noise values are given in Table 1, and contour levels are a geometric progression in factors of 2, starting at 2σ , in this and all subsequent images.

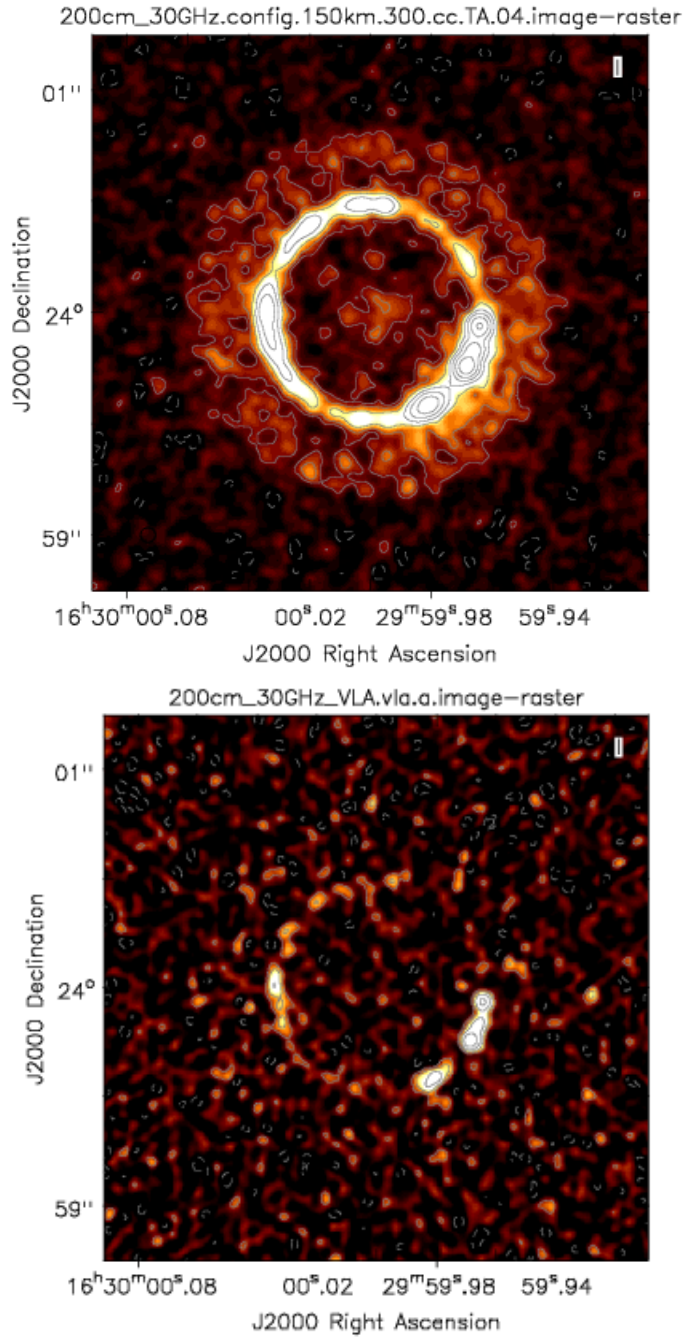


Figure 3: Simulated images at 30GHz of the Barge et al. protoplanetary disk model at a 140pc distance. Top: The Next Generation Very Large Array image tapered to JVLA resolution. Bottom: The Jansky Very Large Array A array image at 60mas resolution.

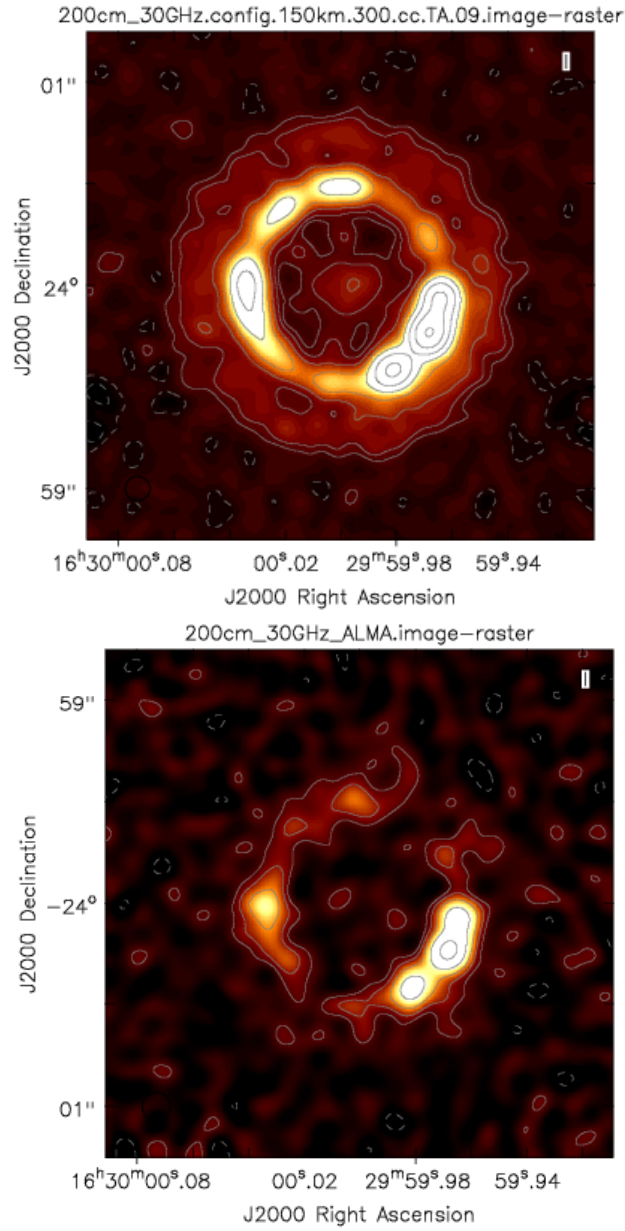


Figure 4: *Simulated images at 30GHz of the Barge et al. protoplanetary disk model at a 140pc distance. Top: The Next Generation Very Large Array image tapered to ALMA resolution. Bottom: The ALMA out28 image at 130mas resolution using Band 1.*

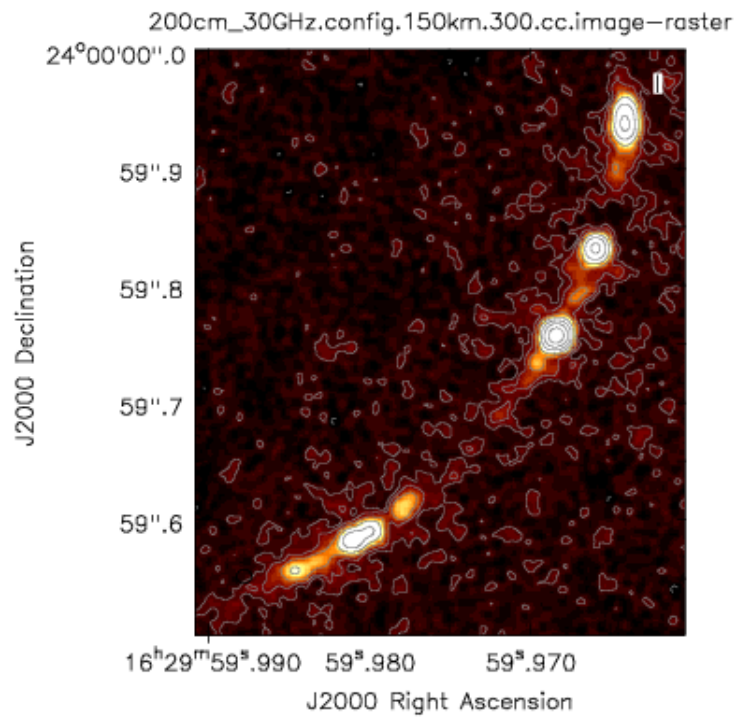


Figure 5: *Blow-up of the arc region of the protoplanetary disk image from the ngVLA at 30GHz, 12mas resolution. The rms noise is 40nJy beam^{-1} .*

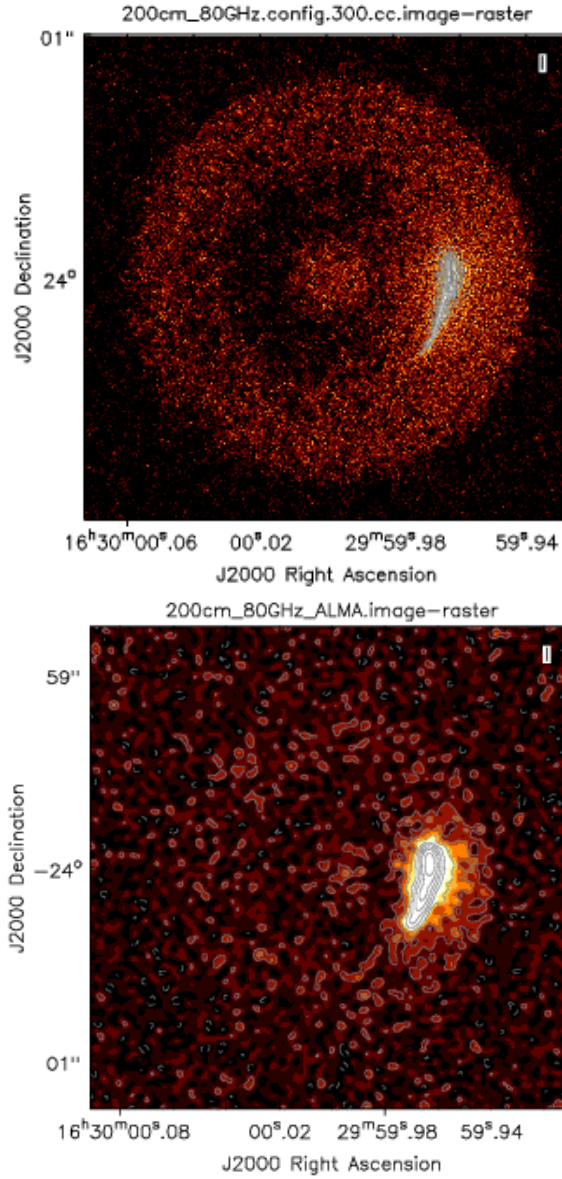


Figure 6: *Simulated images at 80GHz of the Barge et al. protoplanetary disk model at a 140pc distance. Top: The Next Generation Very Large Array image at 5mas resolution. Bottom: The Atacama Large Millimeter Array out28 configuration image of the disk at 50mas resolution. In all cases, the integration time is 100hours. The rms noise values are given in Table 1, and contour levels start at 2σ .*

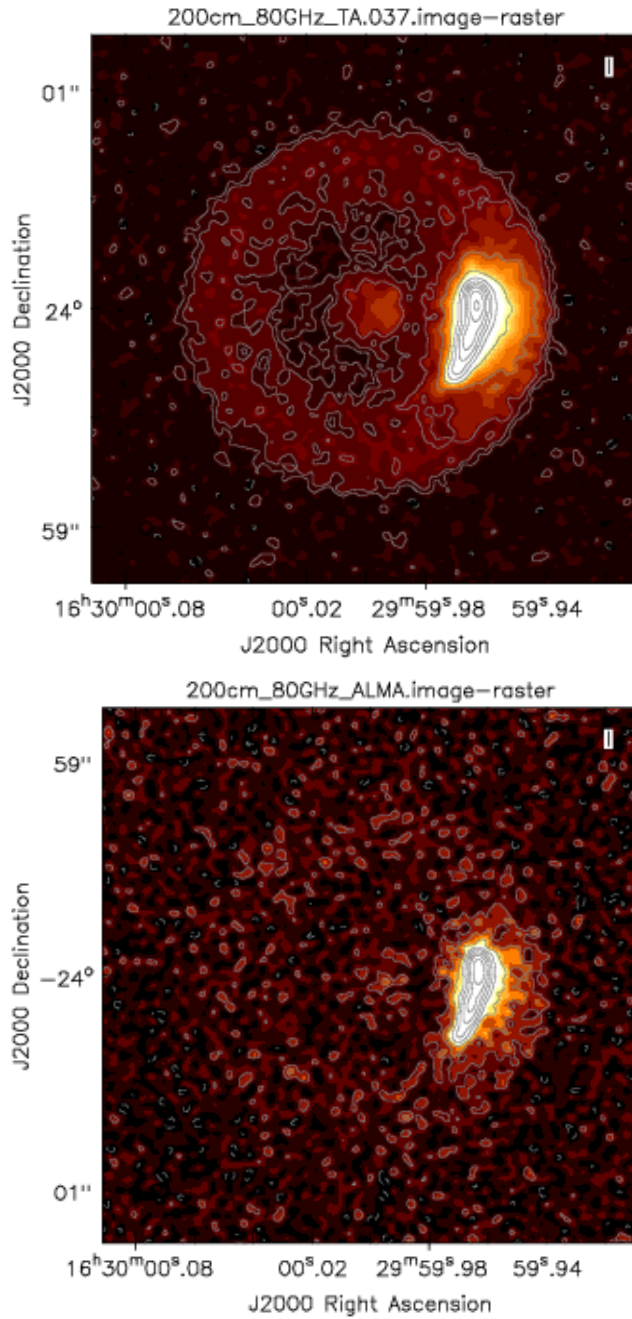


Figure 7: *Simulated images at 80GHz of the Barge et al. protoplanetary disk model at a 140pc distance. Top: The Next Generation Very Large Array image tapered to ALMA resolution. Bottom: The ALMA out28 configuration image at 50mas resolution.*

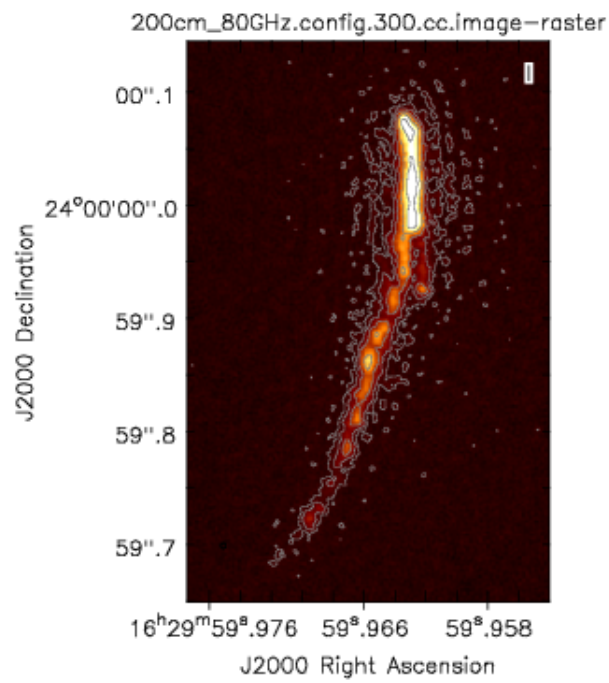


Figure 8: *Blow-up of the arc region of the protoplanetary disk image from the ngVLA at 80GHz, 5mas resolution, with an rms noise of $0.11\mu\text{Jy beam}^{-1}$*

The National Radio Astronomy Observatory and Green Bank Observatory are facilities of the U.S. National Science Foundation operated under cooperative agreement by Associated Universities, Inc. This work was supported by awards AST-2034328 (MSIP Prototype Antenna) and AST-2334267 (ngVLA Design Activities); NRAO related activities are funded under award AST-1647378 (NRAO Operations/Development).

